

A New Texture Descriptor Using Multifractal Analysis in Multi-orientation Wavelet Pyramid *

Yong Xu¹, Xiong Yang¹, Haibin Ling² and Hui Ji³

¹School of Computer Science & Engineering, South China Univ. of Tech., Guangzhou 510006, China

²Department of Computer and Information Sciences, Temple University, Philadelphia, PA 19122, U.S.A.

³Department of Mathematics, National University of Singapore, Singapore 117542

{yxu@scut.edu.cn, xiong.yang@mail.scut.edu.cn, hbling@temple.edu, matjh@nus.edu.sg}

Abstract

Based on multifractal analysis in wavelet pyramids of texture images, a new texture descriptor is proposed in this paper that implicitly combines information from both spatial and frequency domains. Beyond the traditional wavelet transform, a multi-oriented wavelet leader pyramid is used in our approach that robustly encodes the multi-scale information of texture edgels. Moreover, the resulting texture model shows empirically a strong power law relationship for nature textures, which can be characterized well by multifractal analysis. Combined with a statistics on affine invariant local patches, our proposed texture descriptor is robust to scale and rotation changes, more general geometrical transforms and illumination variations. In addition, the proposed texture descriptor is computationally efficient since it does not require many expensive processing steps, e.g., texton generation and cross-bin comparisons, which are often used by existing methods. As an application, the proposed descriptor is applied to texture classification and the experimental results on several public texture datasets verified the accuracy and efficiency of our descriptor.

1. Introduction

Texture analysis is an important problem in computer vision with many applications, e.g., image and scene classification, medical imaging diagnosis. One key property of a desired texture descriptor is its robustness to environment changes including both geometrical and photometric changes ([32]). A good texture descriptor should have strong invariance to many factors, e.g., non-rigid surface deformation, viewpoint changes, illumination variation, ro-

tation, scaling and occlusion. There have been extensive studies on texture descriptors robust to various environmental changes. Most recent works on texture representation are based on the statistical analysis of textons in spatial domain (e.g., [5, 3, 12, 14, 17, 25, 28]), and the main statistical tool they used is the histogram and its variations. Fractal analysis has recently been proposed as a replacement to histogram to better capture the spatial distribution properties of textons ([24, 29, 30]) with impressive results. Meanwhile, there also have been studies on texture analysis in spectral domain, especially with the invention of wavelet transform (e.g., [1, 2, 7]). However, the performance of these wavelet-based texture descriptions is usually less impressive when compared to the start-of-the-art performances ([26, 27]). Despite the great advances in texture analysis, there are always needs for more robust and more computationally efficient texture descriptors.

As [18] demonstrated in their work on scene recognition, the spectral information of texture images contains very important information about textures, and should be included in the description just as the spatial information does. Thus, this paper aims at developing an efficient and robust texture descriptor by combining the analysis in both spatial and spectral domain. The basic underlying idea is applying multifractal analysis to both the low-pass and high-pass wavelet coefficients of textures, as well as a so-called wavelet leaders field derived from high-pass wavelet coefficients of textures. Furthermore, an extra module is developed to achieve better scale invariance of the resulting descriptor by using the statistics on affine invariant local patches. The key components in the proposed method are listed as follows.

Multi-orientation wavelet representation. It is known that wavelet coefficients of texture images include both low-frequency information and multi-scale high-frequency information. However, certain statistical measurements directly on wavelet coefficients could be not very stable as most wavelet coefficients of images tend to be small,

*Project supported by Program for New Century Excellent Talents in University(NCET-10-0368), Chinese Universities Scientific Fund(SCUT 2009ZZ0052) and National Nature Science Foundation of China (60603022).

e.g., negative-order statistical moment which is encoded in multi-fractal analysis. Thus, in addition to traditional wavelet coefficients, a modified version of the so-called *wavelet leaders* [10] technique is incorporated as one part of the underlying representation of textured images, that has been used for facilitating the computation of multi-fractal spectrum of images ([26, 27]). Moreover, the orientation sensitivity of wavelet transform is suppressed in our implementation by leveraging the wavelet coefficients over multiple oriented instances of texture images. In a summary, we propose a wavelet pyramid with multiple orientations which is more stable for statistical computation and encodes multi-scale and multi-orientation information regarding edgels in texture images.

Multifractal analysis. Based on the proposed wavelet pyramid, an MFS (multifractal spectrum) is estimated for each individual component in the wavelet pyramid: low-frequency component, high-frequency component and wavelet leaders. The ultimate texture descriptor is then the combination of all multifractal spectra. Applying multifractal analysis on texture analysis is not a completely new idea (See [29, 30]). However, our approach is different from the existing ones as the multifractal analysis is done on a wavelet pyramid. The advantages of our approach are verified in the experiments of texture classification.

Scale normalization The last component is to address the robustness of the MFS obtained above to scale changes. Motivated by recent progresses in invariant feature detection (*e.g.* [9]), we propose to normalize the given texture images based on the estimate of the texture scales, determined by some statistics of local invariant patches. In our approach, the Laplacian blob detector ([9]), which is affine invariant, is used to collect scales of local patches, followed by a global scale estimation on the whole texture image.

There are two main contributions in our proposed approach. The first is the multifractal analysis in a multi-orientation wavelet pyramid with three components: low-frequency, high-frequency and wavelet leaders. The second is the incorporation of global scale identification for increasing the scale robustness of the proposed MFS. Compared to previous work, the proposed texture descriptor enjoys several advantages, including (1) robustness to geometric transformation and photometric variations (due to MFS), (2) better numerical stability for computing MFS and richer information, provided by the multi-orientation wavelet pyramid, (3) better robustness to global scale changes, and (4) efficient computation as there is no need for expensive texton analysis and cross-bin computation. The proposed texture descriptor is applied to texture classification tasks and the experimental results on several texture datasets show its promising performance against several existing state-of-the-art methods.

The rest of this paper is organized as follows: Sec. 1.1

gives a very brief review on the related work. Sec. 2 is devoted to the introduction of the wavelet transform, wavelet leader and MFS. A detailed description of our texture descriptor is given in Sec. 3. The experimental evaluation of the proposed descriptor is given in Sec. 4. Finally, Sec. 5 concludes the paper.

1.1. Related work and our work

In recent years, methods for texture representation are mostly done in spatial domain, which usually rely on local or global descriptors that are robust to geometric or illumination changes (*e.g.*, [5, 3, 12, 14, 17, 25, 28]). The popular methodology is first extracting local patches through robust feature detectors or randomly sampling. Then these patches are quantized into a texton dictionary and some statistics (mostly histogram based) are built on texton dictionary. For example, Lazebnik et al. [13] proposed a texture description based on the histogram of affine-invariant regions. The good performance of their work is demonstrated in texture classification and retrieval, with the robustness to rotation, scale changes, and affine transformation. However, the histogram does not capture some important statistical properties of the texton dictionary, as it only counts the frequency of the textons. As a replacement to histogram, multifractal analysis is used by Xu et al. [29, 30] for texture analysis. In their work, the pixels are first partitioned into different sets either based on the density function or based on the local orientation template. Then the fractal dimension for each pixel set is estimated and combined together to be a global statistical characterization on all pixels.

There also exist quite a few texture descriptors done in frequency domain, especially in wavelet domain (*e.g.* [2, 6, 7, 26, 27]). Do et al. [7] used the marginal distribution of wavelet coefficients to design a method of texture retrieval. Arivazhagan et al. [1] used more advanced statistical features extracted from both low-frequency and high-frequency components of DWT (discrete wavelet transform) for texture classification. Arneodo et al. [2] proposed the Modulus Maxima of a Continuous Wavelet Transform (MMWT), which is computationally demanding and difficult to implement. Wendt et al. [26, 27] derived a promising texture descriptor based on the so-called wavelet leaders, that are defined on high-frequency wavelet coefficients. Three statistical measurements are defined from the wavelet leaders in their approach: scaling exponents, multi-fractal spectrum and hölder exponents. Although the multifractal analysis is robustly estimated in [26, 27], some important texture primitives are missing in their approaches, also it suffers from the sensitivities to rotation changes and scale changes. Overall, the performance of all these wavelet-based approaches on many tasks such as texture classification is not up to the bar of the state-of-art approaches done in spatial domain yet.

Our proposed work is mainly motivated by the robustness of wavelet leader-based multifractal analysis in [26, 27] and rich informative description on texon distribution provided by multifractal analysis ([29, 30]). In our proposed approach, a multi-orientation wavelet pyramid is used as the representation of texture images which combined both regular wavelet coefficients and wavelet leaders under multiple oriented instances of texture images. Such a wavelet pyramid provides a solid foundation for multifractal analysis with rich information. With the help of an extra module of identifying global scale changes, the resulting multifractal analysis defined on the scale-normalized texture images provides a texture descriptor with stronger robustness to geometrical changes and photometric changes.

2. Wavelets, wavelet leaders and multifractal analysis

Wavelets. There have been extensive literatures on wavelet and its applications; in this paper we only present the basic results related to our work. Interested readers are referred to [15] for more details. Given an image I , its DWT (discrete wavelet transform) decomposes I into one low-frequency channel $D_J(I)$ under the coarsest scale and multiple high-frequency channels under multiple scales $W_{k,j}(I)$, $k = 1, 2, 3$, $j = 1, 2, \dots, J$, where J is the number of scales ($J = 3$ is used in our work). Thus, we have three high-frequency channels ($k = 1, 2, 3$) at each scale j , that encode the discontinuities of the image along horizontal, vertical and diagonal directions. The tensor product of Daubechies' "DB2" wavelet ([15]) is used in our implementation.

Wavelet leaders. For each orientation θ , the *wavelet leaders* ([26, 27]) is defined as the maximum response of all wavelet coefficients in both its spatial neighborhood and its scale neighborhood at smaller scales. In other words, for a wavelet coefficient $W_{k,j_0,\theta}(\vec{r}_0)$ at pixel \vec{r}_0 , its corresponding wavelet leader is defined as

$$L_{j_0,\theta}(\vec{r}_0) = \max_{1 \leq j \leq j_0} \max_{1 \leq k \leq 3} \max_{\vec{r} \in \Omega(\vec{r}_0)} |W_{k,j,\theta}(\vec{r})|, \quad (1)$$

where $\Omega(\vec{r}_0)$ is the square neighborhood centering at \vec{r}_0 .

Fig. 1 and Fig. 2 show examples of wavelets and wavelet leaders. It is seen that a large amount of small wavelet coefficients are removed when converting wavelet coefficients to wavelet leaders, which allows more statistical measurement applicable to the data, *e.g.* the negative-order moment. Such statistical measurement is implicitly used when we estimate multifractal spectrum. On the other hand, such a conversion does not remove too much information of texture images thanks to the multi-scale maximum nature of the edgels in wavelet domain (See [27] for more details).

Multifractal analysis. As a generalization of fractal dimension ([16]), multifractal analysis is a powerful tool to

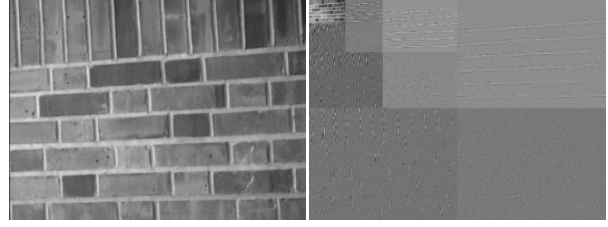


Figure 1. The image and its wavelet coefficients. Left: an image in [22]. Right: its wavelet coefficients (three levels) of the image.

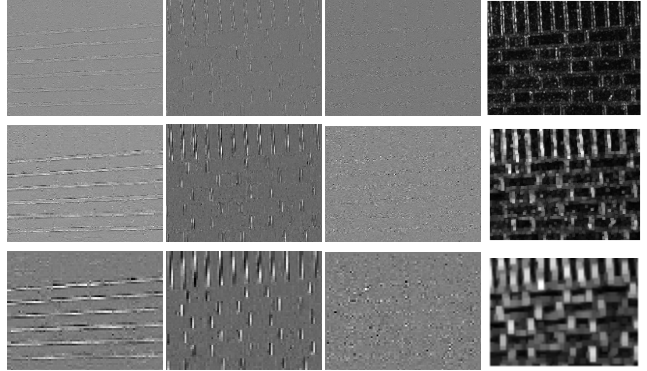


Figure 2. The high-frequency coefficients and wavelet leaders. From left to right in every row, there are wavelet coefficients of horizontal, vertical, diagonal direction and wavelet leader.

describe the irregular 2D functions. The plain fractal dimension is used as a statistical measurement on how a given point set E appears to fill space when one zooms in to finer scales (See [16] for more details). One popular definition of the fractal dimension is the so-called *box-counting* fractal dimension which is defined as follows. Let the 2D space be covered by a mesh of $n \times n$ squares. Given a point set $E \subset R^2$, let $\#(E, \frac{i}{n})$ be the number of $\frac{i}{n}$ -mesh squares that intersect E for $i = 1, 2, \dots$. Then the fractal dimension $dim(E)$ of E ([8]) is defined as

$$dim(E) = \lim_{n \rightarrow \infty} \frac{\log \#(E, \frac{1}{n})}{-\log \frac{1}{n}}.$$

In practice, as the resolution is limited, we estimate the slope of $\log \#(E, \frac{i}{n})$ with respect to $-\log \frac{i}{n}$ for $i = 1, 2, \dots, m$ ($m \leq n$) using the least squares method.

Multifractal analysis generalizes the fractal dimension to characterize the irregularity of functions. Multifractal analysis divides the space into multiple point set E_α according to some categorization term α . For each point set E_α , which is the collection of all points with the same α , let $dim(E_\alpha)$ denote its fractal dimension. The MFS is then given by the multifractal function $dim(E_\alpha)$ vs. α . In the classical definition of the MFS, the categorization term α is defined by the density function (See [31] for more details).

3. Our proposed texture descriptor

Our proposed texture descriptor can be briefly described as the collection of MFS defined on multiple components of a multi-orientation wavelet pyramid which includes both wavelet coefficients and wavelet leaders. The computation of the proposed descriptor is outlined in Algorithm 1. In the rest of this section, we will give detailed description of each step in the algorithm.

Algorithm 1 Texture Description

- 1: Input: texture image I
- 2: Output: descriptor \mathbf{t}
- 3: Scale-normalize image I using the scale estimated from local affine invariant patches (Sec. 3.1)
- 4: Compute the multi-orientation wavelet pyramid: low-frequency wavelets $D(I)$, multi-orientation wavelets $W(I)$ and wavelet leaders $L(I)$ (Sec. 3.2):

$$\{D_{J,\theta}, W_{k,j,\theta}, L_{j,\theta}\} \quad (2)$$

- 5: Compute the MFS for each component in (2) using the box-counting method (Sec. 3.3):

$$\{\text{MFS}(D_\theta), \text{MFS}(W_{k,\theta}), \text{MFS}(L_\theta)\} \quad (3)$$

- 6: $\mathbf{t} \leftarrow$ fusion of (3) (Sec. 3.3)
-

3.1. Scale estimation and normalization

Intuitively, the global scale of a texture pattern affects all its local regions. While direct estimation of global scale can be very unstable, the statistics of scale information drawn from local invariant patches is usually more reliable. Based on this observation, we propose to estimate the texture scale from local patches. Many robust patch or keypoint detectors have been presented recently with scale and affine invariants. For example, Garding and Lindeberg [9] proposed the Laplacian blob detector. By using an affine adaptation process based on the second moment matrix, the ellipse regions obtained from Laplacian blobs become affine invariant. An iterative approach [11] showed that the second moment matrix matches the true shape of the local region, so we can get approximate scale ratios for intra-class textures from the sum of area of these ellipses.

Fig. 3 shows examples of the scale normalization process. In Fig. 3(a), the scale ratios of the three images are roughly 1:1:2, which are computed according to the sum area of detected local ellipses shown in (b). We enlarge the first and second image twice according to this estimation, and the result is shown in (c), where we can see that the normalization effectively makes the three images almost in the same scale.

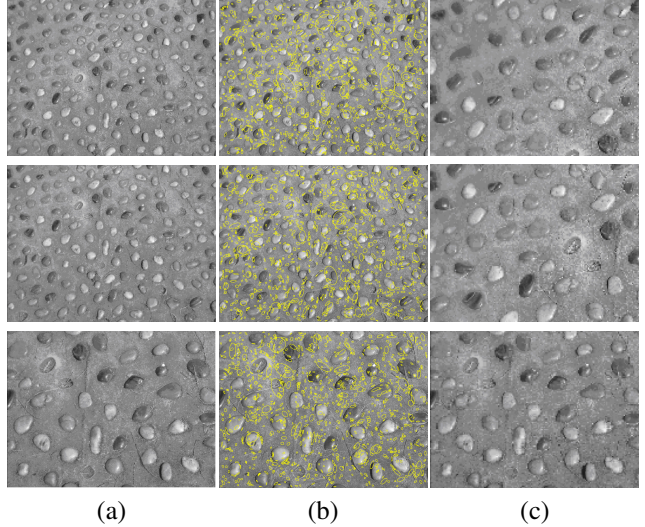


Figure 3. (a) Three textures in different scale, the texture images in the first row and the second row in (a) are nearly in the same scale. (b) One thousand randomly sampled ellipses obtained by using Laplacian blob detector. (c) Enlarge twice the first and the second images in (a), and the third remains unchanged, see Sec. 3.1 for details.

3.2. Multi-orientation wavelet pyramid

It is well-known that the orientation selectivity is quite limited for regular wavelet transform. Thus, we run multiple instances of wavelet transforms with different orientations to improve the orientation selectivity of wavelet transform, which could be equivalently done by applying standard wavelet transform on image rotated with different angles. Specifically, given an input image, we have the following multi-orientation wavelet coefficients and wavelet leaders:

$$\{D_{J,\theta}, W_{k,j,\theta}, L_{j,\theta}\}$$

with $k = 1, 2, 3; j = 0, 1, \dots, J; \theta = 0, 2\pi\frac{1}{N}, \dots, 2\pi\frac{N-1}{N}$, where $D_{J,\theta}(I)$ is the low-frequency wavelet component of scale-normalized image under the coarsest scale J with orientation θ ; N is the number of orientations; $W_{k,j,\theta}(I)$ are three high-frequency component of wavelet transform and $L_{j,\theta}$ is the wavelet leader transform defined in (1).

3.3. Wavelet-based MFS

As described in previous subsections, for an input texture image I , we propose a multi-orientation wavelet pyramid for the scale-normalized texture image. Then we calculate the MFS for each component of wavelet pyramid using the box-counting method, the same as [31] does. Thus, we get the bag of MFS for the given texture image I as follows:

$$\{\text{MFS}(D_{J,\theta}); \text{MFS}(W_{k,j,\theta}); \text{MFS}(L_{j,\theta})\}. \quad (4)$$

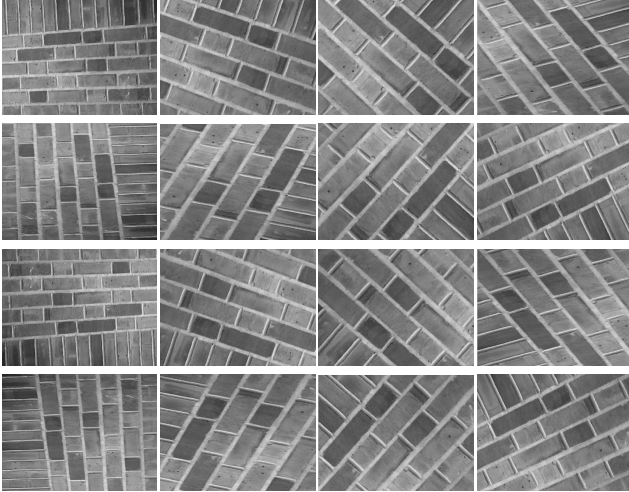


Figure 4. The rotated texture image set for 16 uniformly sampled orientations.

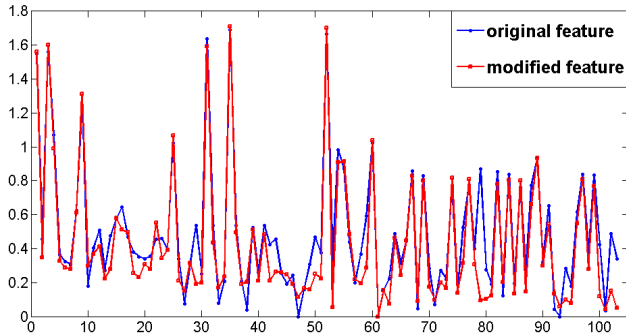


Figure 5. The blue curve shows the feature of the original texture image; the red curve shows the mean of features of 16 texture images in Fig. 4. The x-axis denotes the 103-dimension vector, and the y-axis denotes the fractal dimension.

Instead of directly using such a bag of MFS as our texture descriptor, we define our wavelet-based MFS (WMFS) by leveraging the MFS over its multiple instances of orientation, i.e.

$$\text{WMFS} = \{ \text{mean}_{\theta}(\text{MFS}(D_{J,\theta})), \text{mean}_{\theta}(\text{MFS}(W_{k,j,\theta})), \text{mean}_{\theta}(\text{MFS}(L_{j,\theta})) \}. \quad (5)$$

The motivation of averaging over orientations is for the strong robustness of the resulting descriptor to global rotation.

In summary, for each coefficient matrix, we get a 26-dimension MFS feature using the algorithm in [31]. Since three scales are used (i.e., $J = 3$), there are 13 wavelet coefficient matrices, including low- and high-pass components and wavelet leaders. Thus the texture feature is $26 \times 13 = 338$ dimensional. In this paper, we conduct feature selection ([4]) on the 338 features and get an optimal 103-dimension

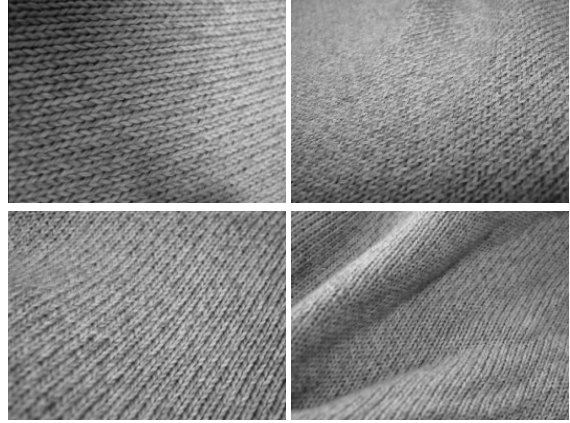


Figure 6. Four fabric texture F1, F2, F3, F4, including rotation, viewpoint, scale, illumination and non-rigid surface changes.

texture representation. Fig. 4 and Fig. 5 show the process of averaging over orientations.

Fig. 6 shows four texture images (in [22]) from the same texture class under different rotation, viewpoint, scale, illumination and non-rigid surface changes. Fig. 7(a) shows that their feature vectors extracted by our method are nearly identical. For comparison, Fig. 7(b) shows their feature curves extracted by the method without the scale and rotation processing.

4. Experimental evaluation

We evaluated the performance of the proposed texture descriptor on the texture classification task. Two public datasets are tested: one is from UIUC ([22]) and the other is from UMD ([23]). The UIUC texture dataset consists of 1000 uncalibrated, unregistered images: 40 samples for each of 25 textures with a resolution 640×480 pixels, and the UMD texture dataset consists of 1000 uncalibrated, unregistered images: 40 samples for each of 25 textures with a resolution of 1280×900 pixels. Significant viewpoint changes and scale differences are present in both datasets, and the illumination conditions are uncontrolled.

In our classification experiments, the training set is selected as a fixed size random subset of the class, and all remaining images are used as the test set. The reported classification rate is the average over 200 random subsets. An SVM classifier (Tresp *et al.* [21]) is used in the experiments, which was implemented as in Pontil *et al.* [19]. The features of the training set are used to train the hyperplane of the SVM classifier using RBF kernels as described in Scholkopf *et al.* [20]. The optimal parameters are found by cross-validation.

We compared our method against four methods including Lazebnik *et al.* [11], Varma *et al.* [24], Xu *et al.* [30] and Xu *et al.* [29]. The first one is the (H+L)(S+R) method

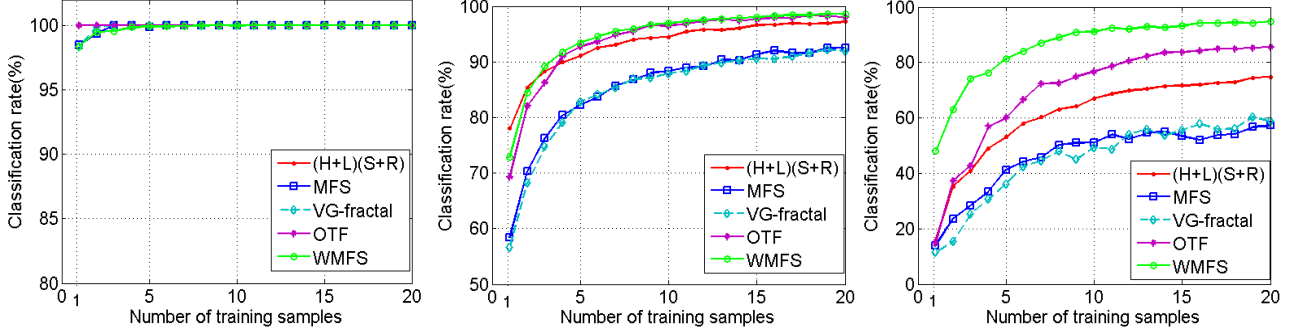


Figure 8. Classification rate vs. number of training samples on UIUC dataset based on SVM classifier. Five methods are compared: the (H+L)(S+R) method in Lazebnik *et al.* [11], the MFS method in Xu *et al.* [30], the VG-Fractal method in Varma *et al.* [24], the OTF method in Xu *et al.* [29] and our WMFS method. Left: classification rate for the best class. Middle: mean classification rate for all 25 classes. Right: classification rate for the worst class.

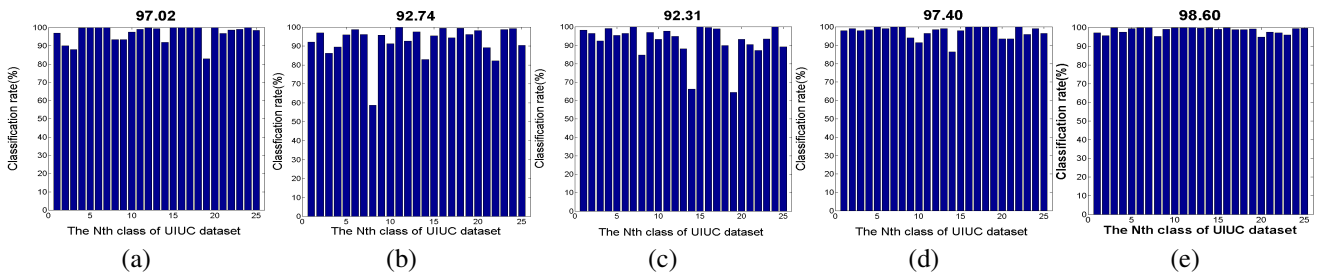


Figure 9. Classification percentage vs. index of classes on UIUC dataset based on SVM classifier. The number of training samples is 20. The number on the top of each sub-figure is the average classification percentage of all 25 classes. (a) Result of the (H+L)(S+R) method. (b) Result of the MFS method. (c) Result of the VG-Fractal method. (d) Result of the OTF method. (e) Result of our WMFS method.

by Lazebnik *et al.* [11], which is based on a sophisticated point-based texture representation. The basic idea is to first characterize the texture by clusters of elliptic regions. The ellipses are then transformed to circles such that the local descriptor is invariant to affine transform. Two descriptors (SPIN and RIFT) are defined on each region. The resulting texture descriptor is the histogram of clusters of these local descriptors, and the descriptors are compared using the EMD distance. The second method is the VG-fractal method by Varma and Garg [24], which use properties of the local variance function of various image measurements resulting in a 13 dimensional descriptor. The resulting texture descriptor is the histogram of clusters of these local descriptors. The third method is the MFS method by Xu *et al.* [30]. In [30] the pixel classification is based on the local density function at each point. In total three local density functions based on image intensity, image gradient and image Laplacian were defined, and the texture descriptor is obtained by combining the three MFSs based on the corresponding pixel classification. The fourth method is the OTF method by Xu *et al.* [29]. The pixel classification is based on the MFS which is based on local orientation histograms under multiple neighborhood sizes, which makes the feature robust to illumination changes and local geometric changes.

Thus the texture representation has strong invariance to both illumination changes and environmental changes. Furthermore, the MFSs were projected into a tight frame system to enhance the invariance to large scale changes. Our proposed WMFS texture descriptor is based on the combination of wavelet transform and MFS, and the invariances of scale and rotation are also addressed in our proposed descriptor.

The results on both UIUC dataset and UMD dataset are from [29]. Denote the proposed approach as WMFS method. Fig. 8 shows the classification rate vs. the number of training samples on the UIUC dataset. Fig. 9 shows the classification percentage vs. the index of classes on the UIUC dataset based on 20 training samples. Fig. 10 and Fig. 11 show the same experiments for the UMD dataset. From Fig. 8 to Fig. 11, it is seen that the WMFS method clearly outperformed all the other methods on both UIUC and UMD datasets. Moreover, our method is efficient and practical due to the low computational cost of DWT and MFS, and the dimension of our descriptor is also low. Table 1 shows the classification accuracy of different method on UIUC dataset, and Table 2 shows the classification accuracy of different method on UMD dataset. The numbers of training images per class are 5,10,15 and 20 respectively.

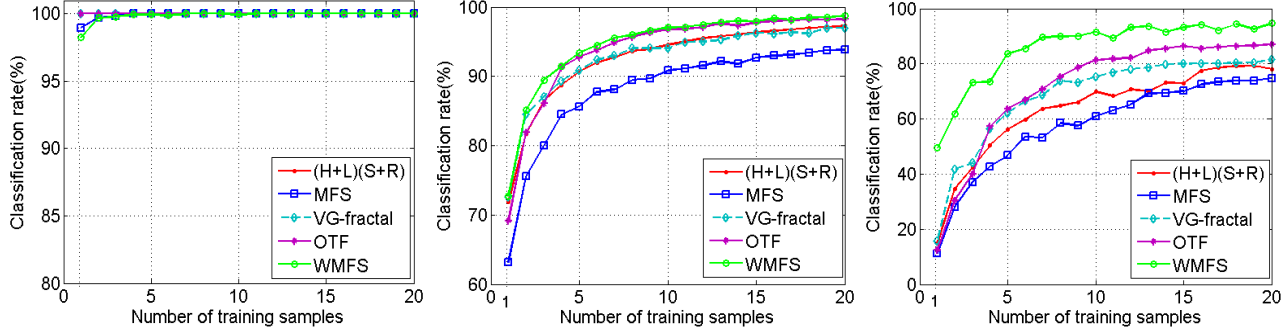


Figure 10. Classification rate vs. number of training samples on UMD dataset based on SVM classifier. Five methods are compared: the (H+L)(S+R) method, the MFS method, the VG-Fractal method, the OTF method and our WMFS method. Left: classification rate for the best class. Middle: mean classification rate for all 25 classes. Right: classification rate for the worst class.

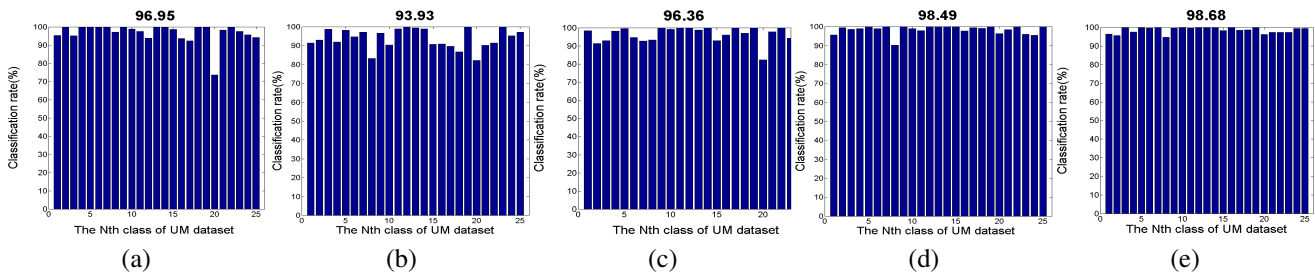


Figure 11. Classification percentage vs. index of classes on UMD dataset based on SVM classifier. The number of training samples is 20. The number on the top of each sub-figure is the average classification percentage of all 25 classes. (a) Result of the (H+L)(S+R) method. (b) Result of the MFS method. (c) Result of the VG-Fractal method. (d) Result of the OTF method. (e) Result of our WMFS method.

method	5	10	15	20
VG-fractal	82.86	87.85	90.62	92.31
MFS	82.24	88.36	91.38	92.74
(H+L)(S+R)	91.12	94.42	96.64	97.02
OTF	92.75	96.48	96.97	97.40
WMFS	93.42	96.95	98.01	98.60

Table 1. Classification accuracy of different methods on UIUC dataset.

method	5	10	15	20
VG-fractal	90.92	94.09	96.22	96.36
MFS	85.63	90.82	92.67	93.93
(H+L)(S+R)	90.71	94.54	96.29	96.95
OTF	92.82	96.81	97.78	98.49
WMFS	93.40	97.05	97.92	98.68

Table 2. Classification accuracy of different methods on UMD dataset.

5. Summary and conclusions

In this paper we proposed a texture descriptor based on the MFS defined on a multi-orientation wavelet pyramid including low-frequency and high-frequency wavelet compo-

nents and wavelet leaders. The proposed texture descriptor is robust to many environmental changes and encodes rich information of textures. Moreover, the scale invariance of the proposed descriptor is further enforced by a scale-normalization pre-process using affine invariant regions detected by Laplacian blob detector, and the rotation invariance is also improved by leveraging MFS over multiple instances of oriented images. The experiments showed that our texture descriptors perform excellently for texture classification on several public texture datasets.

References

- [1] S. Arivazhagan and L. Ganesan, "Texture Classification Using Wavelet Transform," *Pattern Recognition Letters*, 24, pp. 1513-1521, 2003.
- [2] A. Arneodo, N. Decoster, P. Kestener and S. Roux, "A Wavelet-based Method for Multifractal Image Analysis: From Theoretical Concepts to Experimental Applications," *Advances in Imaging and Electron Physics*, 126, pp. 1-98, Academic Press, 2003.
- [3] B. Caputo, E. Hayman, M. J. Fritz, J. O. Eklundh, "Classifying Materials in the Real World", *Image and Vision Computing*, 28, pp. 150-163, 2010.
- [4] Y.W. Chen and C.J. Lin, *Combining SVMs with various feature selection strategies*, Springer, 2006.

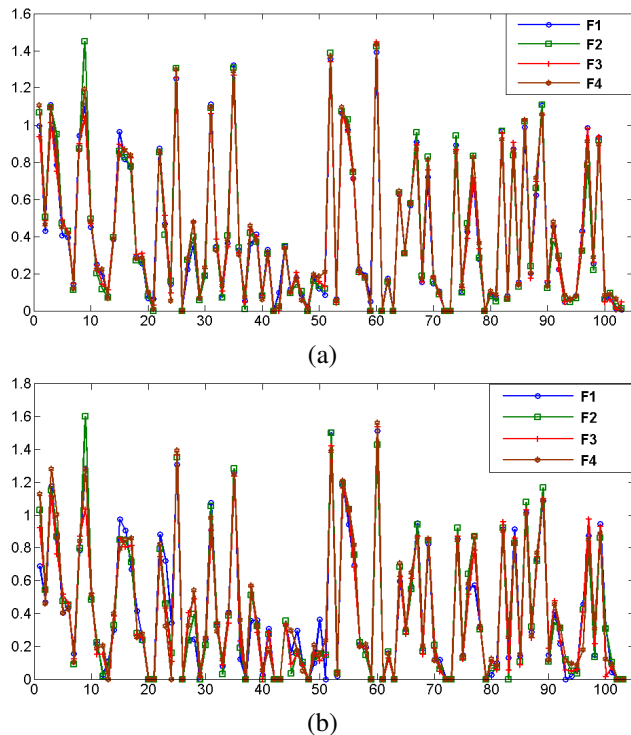


Figure 7. Feature vectors of textures shown in Fig. 6. The x-axis denotes the 103-dimension vector, and the y-axis denotes the fractal dimension. (a) The feature vectors extracted by our method; (b) The feature vectors extracted by our method without scale and rotation processing.

- [5] K. Dana and S. Nayar, "Histogram Model for 3d Textures", *CVPR*, pp. 618-624, 1998.
- [6] J.S. De Bonet and P. Viola, "Texture Recognition Using a Non-parametric Multi-Scale Statistical Model", *CVPR*, 1998.
- [7] M.N. Do and M. Vetterli, "Wavelet Based Texture Retrieval Using Generalized Gaussian Density and Kullback-Leibler Distance," *IEEE Trans. Image Processing*, 146-158, 2002.
- [8] K. J. Falconer, *Techniques in Fractal Geometry*, John Wiley, 1997.
- [9] J. Garding and T. Lindeberg, "Direct Computation of Shape Cues Using Scale-adapted Spatial Derivative Operators," *IJCV*, 17(2), pp. 163-191, 1996.
- [10] B. Lashermes, S. Jaffard and P. Abry, *Wavelet leader based multifractal analysis*, ICASSP, 2005.
- [11] S. Lazebnik, *Local Semi-local and Global Models for Texture, Object and Scene Recognition*, Ph.D. Dissertation, University of Illinois at Urbana-Champaign, 2006.
- [12] S. Lazebnik, C. Schmid and J. Ponce, "A Discriminative Framework for Texture and Object Recognition Using Local Image Features," In *Toward Category-Level Object Recognition*, Springer-Verlag LNCS, 2006.
- [13] S. Lazebnik, C. Schmid and J. Ponce, "A Sparse Texture Representation Using Affine-invariant Regions," *PAMI*, 8(27), pp. 1265-1278, 2005.
- [14] T. Leung and J. Malik, "Representing and Recognizing the Visual Appearance of Materials Using Three-dimensional Textons", *IJCV*, 43(1), pp. 29-44, 2001.
- [15] S. Mallat, *A Wavelet Tour of Signal Processing*, Academic Press, CA:San Diego, 1998.
- [16] B. B. Mandelbrot, *The Fractal Geometry of Nature*, San Francisco, CA: Freeman, 1982.
- [17] F. Mindru, T. Tuytelaars, L. Van Gool and T. Moons, "Moment Invariants for Recognition Under Changing Viewpoint and Illumination," *CVIU*, 94(1-3):3-27, 2004.
- [18] A. Oliva and A. Torralba, "Modeling the Shape of the Scene: A Holistic Representation of the Spatial Envelope," *IJCV*, 42(3), pp. 145-175, 2001.
- [19] M. Pontil and A. Verri. "Support Vector Machines for 3D Object Recognition", *PAMI*, 20(6), pp. 637-646, 1998.
- [20] B. Scholkopf and A. Smola, *Learning with Kernels: Support Vector Machines, Regularization, Optimization and Beyond*, MIT Press, Cambridge, MA, 2002.
- [21] V. Tresp and A. Schwaighofer, "Scalable Kernel Systems," *ICANN*, LNCS 2130, pp. 285-291, 2001.
- [22] UIUC: http://www-cvr.ai.uiuc.edu/ponce_grp/data/index.html.
- [23] UMD: http://www.cfar.umd.edu/~fer/High-resolution-database/hr_database.htm.
- [24] M. Varma and R. Garg, "Locally Invariant Fractal Features for Statistical Texture Classification," *ICCV*, 2007.
- [25] M. Varma and A. Zisserman, "Classifying Images of Materials: Achieving Viewpoint and Illumination Independence," *ECCV*, 3, pp. 255-271, 2002.
- [26] H. Wendt, P. Abry, S. Jaffard, H. Ji and Z. Shen, "Wavelet Leader Multifractal Analysis for Texture Classification," *ICIP*, 2009.
- [27] H. Wendt, S.G. Roux, S. Jaffard and P. Abry, "Wavelet Leaders and Bootstrap for Multifractal Analysis of Images," *Signal Processing*, 89(6), pp. 1100-1114, 2009.
- [28] J. Wu and M. J. Chantler, "Combining Gradient and Albedo for Rotation Invariant Classification of 2D Surface Texture", *ICCV*, 2, pp. 848-855, 2003.
- [29] Y. Xu, S.B. Huang, H. Ji and C. Fermuller, "Combining Powerful Local and Global Statistics for Texture Description," *CVPR*, pp. 573-580, 2009.
- [30] Y. Xu, H. Ji and C. Fermuller, "A Projective Invariant for Textures," *CVPR*, 2, pp. 1932-1939, 2006.
- [31] Y. Xu, H. Ji and C. Fermuller, "Viewpoint Invariant Texture Description Using Fractal Analysis," *IJCV*, 83(1), pp. 85-100, 2009.
- [32] S. C. Zhu, Y. Wu and D. Mumford, "Filters, Random Fields and Maximum Entropy (FRAME): Towards a Unified Theory for Texture Modeling", *IJCV*, 27(2), pp. 107-126, 1998.